Observations of the Effect of Rain Temperature on the Surface Heat Flux in the Intertropical Convergence Zone

P. FLAMENT AND M. SAWYER

Department of Oceanography, University of Hawaii at Manoa, Honolulu, Hawaii

14 March 1994 and 20 July 1994

ABSTRACT

The thermohaline response of the ocean to a short (10 h) but intense (95 mm) nighttime rainfall event was observed during a transit through the ITCZ. Two CTD profiles and shipboard measurements of air–sea fluxes were consistent with the assumption that rain temperature equals the wet-bulb temperature, within measurement errors. Although the net freshwater input and the net heat loss inferred from the T–S characteristics of the surface layer were ~30% smaller than those obtained by integrating the measured air–sea fluxes, owing to different spatial sampling, inherent limitations of rain measurement from ship, and contamination by internal waves, the two independent estimates of the net heat deficit agreed remarkably well, within 2.4%, when expressed per unit mass of rain (~72 kJ kg^{-1}). The heat flux due to the temperature of the rain accounted for about 40% of the net heat flux during rain, and therefore cannot be neglected.

1. Introduction

Precipitation is a large component of the surface buoyancy flux in the tropical ocean: a rain rate of 1 cm day^{-1} contributes to the density structure of the upper ocean as much as a heat flux of nearly 40 W m^{-2}, not negligible compared to the buoyancy contribution of the average net heat flux. Precipitation forms a so-called barrier layer of low density water, which inhibits mixing of surface properties deeper into the ocean (Lukas and Lindstrom 1991). This layer traps the heat, freshwater, and momentum fluxes near the surface, retaining a "memory" of the fluxes until a wind event strong enough to erode the stratification occurs.

Precipitation contributes to the buoyancy flux not only through the effect of freshwater on salinity and density but also if the rain temperature is different from the temperature of the ocean. The temperature of freely falling drops is generally believed to be close to the wet-bulb temperature (Kinzer and Gunn 1951; Kincaid and Longley 1989). Gosnell et al. (1993), taking the adiabatic vertical temperature gradient of the air into account, demonstrated that rain temperature would be at most 0.2°C lower than the wet-bulb temperature.

Layers of lower-than-average salinity, formed during heavy precipitation, are in general also colder than average (Ostapoff et al. 1973; Greenhut 1978; Lukas 1990). Recently Bahr and Paulson (1990), measuring salinity and temperature in the equatorial Pacific from a towed catamaran, estimated the rain temperature by extrapolating the T–S diagram of the surface layer to zero salinity. They found an average rain temperature of 21°C, significantly lower than the 24.7°C average wet-bulb temperature, and slightly lower than the 22.6°C minimum wet-bulb temperature. To resolve this apparent controversy, direct measurements of rain temperature were attempted in 1993 during TOGA COARE (Weller 1992, personal communication).

In this paper, observations of the effects of rain temperature during the 1990 Tropical Instability Wave Experiment will be presented. The thermal response of the ocean to a short but intense precipitation event (95 mm over 10 h) will be described, using a combination of satellite images, hydrography, and measurements of air–sea fluxes.

It will be shown that, for the event observed, nearly 40% of the heat deficit of the barrier layer could be attributed to the rain temperature, the remaining mostly to the latent and sensible heat fluxes during the rain period. Rain temperature must be taken into account when computing the net heat flux, but the error made assuming that the rain temperature equals the wet-bulb temperature is negligible compared to other sources of error.

The observations are presented in section 2 and discussed in section 3. Details on the instruments and data processing can be found in the appendix.

2. Observations

The event occurred on 4 September 1990 while the R/V *Moana Wave* was in transit from 2°N, 140°W

Corresponding author address: Dr. Pierre Flament, Department of Oceanography, School of Ocean and Earth Science and Technology, University of Hawaii, 1000 Pope Road, Honolulu, HI 96822.

to Hawaii. Temperatures from the TOGA-TAO mooring at 7°N, 147°30W indicate that, between 1 and 4 September, the atmospheric regime was characterized by strong diurnal convection. The air temperature reached the ~28.5°C sea surface temperature each morning and decreased to often less than 25°C at the onset of precipitation in the early evening. A night time NOAA AVHRR satellite image for 4 September at 1226 UTC is shown in Fig. 1 (local solar time lags UTC by 0935 at the longitude of the observations). The ship track crossed an intense convection cluster at about 9°N, with cells towering at −80°C.

a. *Fluxes inferred from the barrier layer*

At 1220 UTC, a CTD station was done at 8°30N, 143°45W, after nearly 10 h of heavy precipitation. The down and up casts are shown in Fig. 2, and their T–S diagrams are shown in Fig. 3. They were separated by about 40 min in time and 500-m distance over water (the integral of the ship speed from the ADCP). A relic (or fossil) mixed layer of 28.7°C and 34.1 salinity was observed down to 22-m depth, capped by a ~7 m thick layer of water ~0.4 less saline and ~0.2°C colder.

The conservation of salt before and after the rain is expressed as

$$\int_0^D (S(z) - S_0)dz = d(S_r - S_0), \qquad (1)$$

where d is the net freshwater input, $S(z)$ is the measured salinity profile, $S_r = 0$ is the salinity of the rain assumed to be negligible, S_0 is the salinity of the fossil mixed layer, and D is the depth at which $S(D) = S_0$. Solving this equation for the averaged down and up casts gives 61 mm of freshwater input d since the end of the mixing event, which formed the fossil mixed layer.

The conservation of heat before and after the rain is expressed as

$$\int_0^D C_{ps}\rho_s(T(z) - T_0)dz = C_{pr}\rho_r d(T_r - T_0), \qquad (2)$$

where T_0 is the temperature of the fossil mixed layer; $T(z)$ is the measured temperature profile; C_{ps}, C_{pr}, ρ_s,

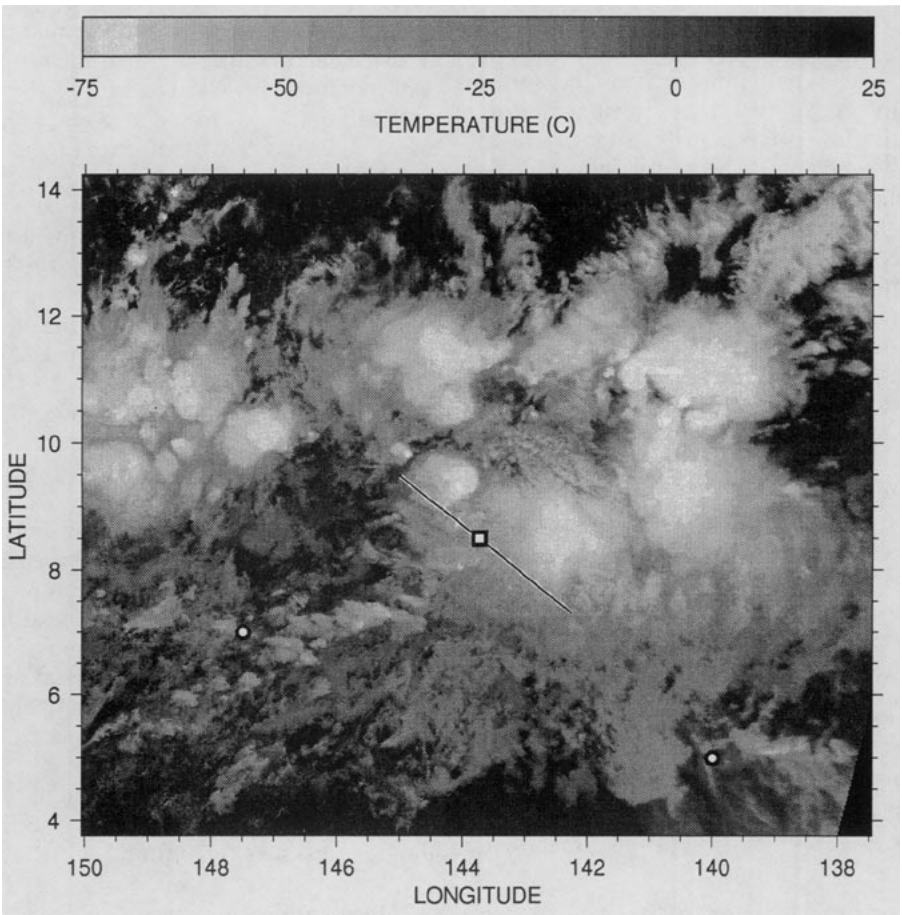

FIG. 1. Thermal infrared image at 1211 UTC 4 September 1990 from satellite *NOAA-11* (10-μm channel). The positions of the TOGA-TAO moorings (●) and of the CTD station (■), and the track of the R/V *Moana Wave* between 0000 and 1700 UTC are shown.

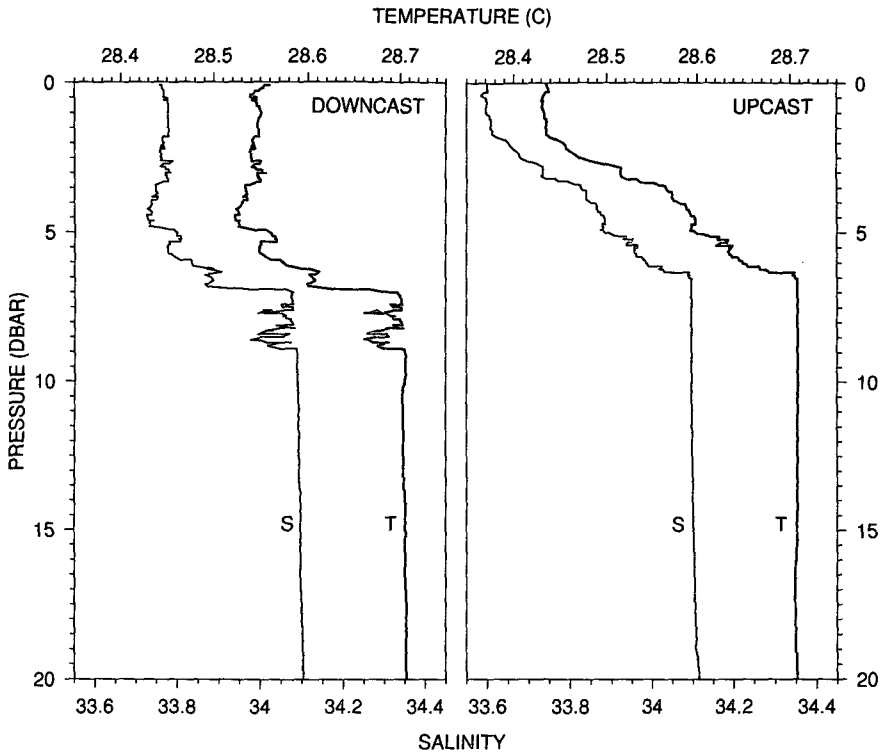

FIG. 2. Profiles of temperature (thick) and salinity (thin) at CTD station 76, 1220 UTC 4 September. Left: up cast; right: down cast.

and ρ_r are the specific heats and density of seawater and freshwater (assumed independent of temperature at T_0); and T_r would be the rain temperature if the other heat fluxes through the sea surface, and the heat fluxes through the base of the mixed layer, were negligible. Solving this equation for the average cast gives 11.2°C for the rain temperature T_r. Expressed per unit mass of rain, this corresponds to a heat deficit $C_{pr}(T_r - T_0) = 73.1$ kJ kg^{-1} and, expressed per unit area, to a heat loss $C_{pr}\rho_r d(T_r - T_0) = -4.40$ MJ m^{-2}.

Mixing by the hull of the ship may have distorted the CTD profiles: during the station, the ship drift measured by the ADCP (20 cm s^{-1}) was about twice the phase speed of interfacial waves estimated from the density profile ($\sqrt{g'h}$ = 11 cm s^{-1}), yielding a supercritical Froude number Fr $\sim$ 2. Mixing may explain the 5-m deep mixed layer and a possible overturn at 8 m observed in the downcast. However, mixing would not modify the left-hand sides of Eqs. (1) and (2) and therefore would not affect the estimation of d and T_r.

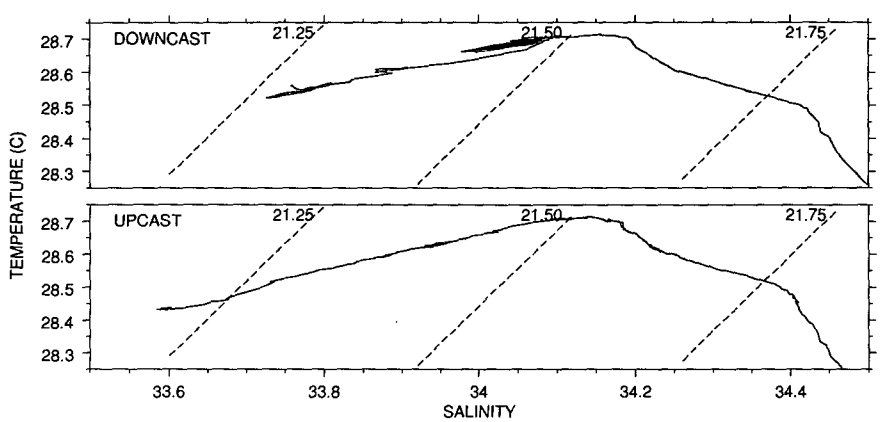

FIG. 3. T–S diagram corresponding to Fig. 2. Isopycnals are shown.

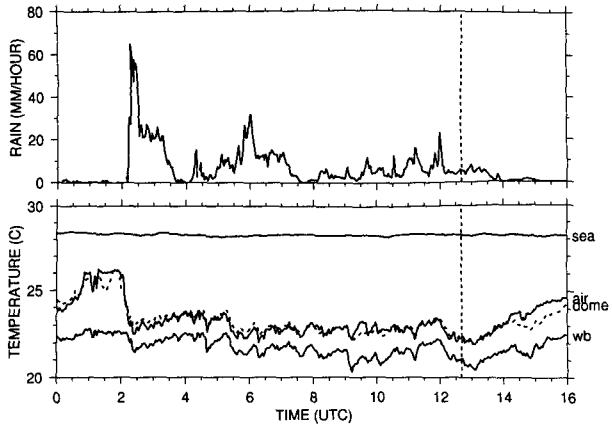

FIG. 4. Upper panel: time series of rain rate; lower panel: time series of surface water (top, solid), air (middle, solid), and wet-bulb temperatures (bottom, solid), and pyrgeometer dome temperature (dotted), along the ship track shown in Fig. 1. The time of the CTD station is shown by a dashed line.

The 11.2°C "rain temperature" estimated from Eqs. (1)–(2) (equivalent to extrapolating the T–S diagram to zero salinity) is unrealistically cold. A freely falling water drop reaches equilibrium at the wet-bulb temperature after a finite time that depends on the size of the drop and the fall speed, but which is typically a few seconds (Kinzer and Gunn 1951; Kincaid and Longley 1989). Even if the adiabatic vertical temperature gradient of the air ($\sim 10^{-2}$ K m^{-1}) is taken into account, the rain temperature is at most 0.2°C colder than the wet-bulb temperature for rain rates up to 100 mm h^{-1} and precipitating cloud heights up to 5000 m (Gosnell et al. 1993).

Figure 4 shows the time series of rain rate measured from the ship for 4 September. Rain started abruptly at 0224 UTC, peaking at 2×10^{-5} m s^{-1} (70 mm h^{-1}) and then decreasing to 3×10^{-6} m s^{-1} (10 mm h^{-1}). Also shown are the time series of sea surface, air, and wet-bulb temperatures, and of the temperature of the pyrgeometer dome, a hemispherical silicon shell ~30 mm in diameter with a thermistor glued on the concave face. When rain started, the air and dome temperatures dropped from 26°C to 23.5°C, and remained ~1.6°C above the wet-bulb temperature within 0.3°C rms until the rain stopped 12 h later. Although the pyrgeometer dome responds in a complex and unknown way to rain, air temperature, humidity, and wind speed, these series indicate that the rain temperature was close to the wet-bulb temperature: had it been much colder, the temperature of the dome would have frequently dropped below the wet bulb. This was never observed.

Assuming that the actual rain temperature was, indeed, at the ~21.9°C average wet-bulb temperature and not at 11.2°C, the heat loss due to the rain temperature was −1.73 MJ m^{-2}, or only 39% of the total heat loss inferred from the CTD. Can the remaining 61% be accounted for by the other air–sea fluxes?

b. *Direct measurements of the fluxes*

The rain rate measured along the ship track (Fig. 4) and integrated until the time of the CTD station is 95 mm. The evaporative flux integrated over the same period is 10 mm, resulting in a net freshwater input of 85 mm.

The time series of the net shortwave, net longwave, latent, sensible, and rain heat fluxes measured along the ship track are shown in Fig. 5 (the computation of these fluxes is discussed in the appendix). Wind speed (not shown) fluctuated around 5 m s^{-1}. The heat flux due to the rain was computed assuming that the rain temperature equals the wet-bulb temperature; that is,

$$H_R = C_{pr}\rho_r \dot{d}(T_{wb} - T_0), \qquad (3)$$

where $\dot{d}$ is the rain rate in m s^{-1}. Note that the rain heat flux H_R reached an astounding −400 W m^{-2} when the rain rate peaked at 70 mm h^{-1}. Due to the decreasing air temperature, the relative importance of the sensible heat flux increased fivefold during the rain: the Bowen ratio H_S/H_L increased from ~0.17 before the rain to an average of 0.81. Figure 6 shows the integral of the fluxes from 0224 UTC, the onset of the rain, until 1240 UTC, the time of the CTD station. The net heat loss inferred from the shipboard sensors was −6.06 MJ m^{-2}. Expressed per unit mass of rain,

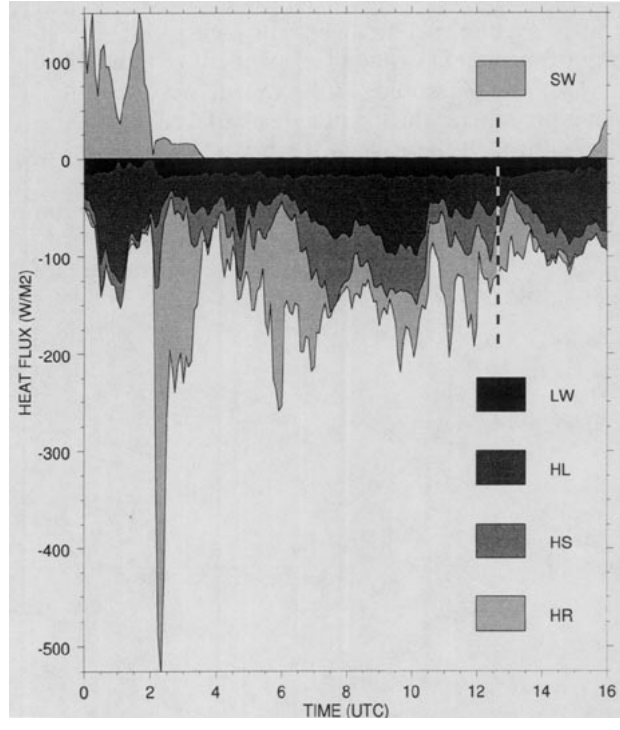

FIG. 5. Cumulative plot of the time series of the net shortwave (*SW*), net longwave (*LW*), latent (*HL*), sensible (*HS*), and rain heat (*HR*) fluxes along the ship track shown in Fig. 1. The time of the CTD station is shown by a dashed line.

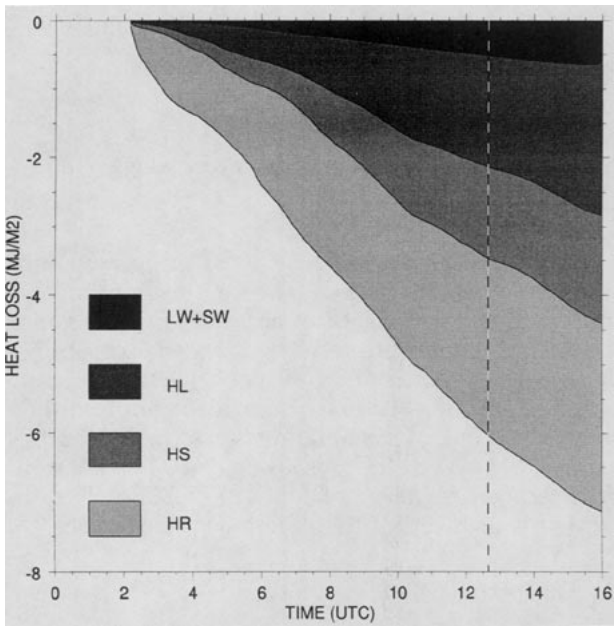

FIG. 6. Heat fluxes integrated from the onset of the rain: rain (*HR*), sensible (*HS*), latent (*HL*), and net radiation (*LW* + *SW*) fluxes. The time of the CTD station is shown by a dashed line.

this corresponds to a total heat deficit of 71.4 kJ kg^{-1}. The net radiation flux (−0.52 MJ m^{-2}), the sensible heat flux (−1.33 MJ m^{-2}), and the latent heat flux (−1.64 MJ m^{-2}) accounted for 58% of the net heat loss. The heat loss due to the rain temperature was −2.57 MJ m^{-2}, or 42% of the net heat loss.

The freshwater input inferred from the shipboard sensors (85 mm) was 1.41 times that inferred from the CTD (61 mm), whereas the net heat loss inferred from the shipboard sensors (−6.06 MJ m^{-2}) was 1.38 times that inferred from the CTD (−4.40 MJ m^{-2}). The smaller values of freshwater input and heat loss inferred from the CTD may easily be attributed to a combination of 1) uncertainties of rain measurements near the structure of a ship (cf. Austin and Geotis 1980), 2) different spatial samplings, the ship integrating over a 175-km track but the barrier layer integrating at the fixed position of the station, and 3) near-surface interfacial/internal waves distorting the thickness of the barrier layer, an inherent limitation to the estimation of fluxes from the near-surface *T*–*S* properties.

However, the ratio of the rain heat flux to the total heat flux did not depend much on the sampling strategy: it was nearly identical whether inferred from the shipboard sensors (42%) or from the CTD (39%), as illustrated in Fig. 7. Expressed per unit mass of rain, the shipboard sensors and the CTD yielded two independent measurements of the heat deficit, 71.4 kJ kg^{-1} and 73.1 kJ kg^{-1}, differing by only 2.4%!

3. Summary and discussion

The thermohaline response of the tropical ocean to a short but intense nighttime rainfall event has been observed. Extrapolation of the *T*–*S* diagrams of two CTD profiles to zero salinity yielded an unrealistic estimate of the rain temperature (11.2°C), indicating that other air–sea fluxes (principally latent heat *HL* and sensible heat *HS*) made a significant contribution to the upper-ocean cooling during the rain. Temperature time series were consistent with the assumption that the rain temperature equals the wet-bulb temperature within measurement errors. With this assumption, the two independent estimates of the net heat deficit, from the *T*–*S* diagram and from the integral of the measured fluxes, agreed within 2.4% when expressed per unit mass of rain. The heat flux due to the temperature of the rain accounted for about 40% of the net heat flux during the rain event.

The surface buoyancy flux due to the rain, obtained by adding the time derivatives of (1) and (2), expressed in density units

$$\int_0^D \dot{\rho}(z)dz = \dot{d}(\partial_S\rho(S_r - S_0) + \tau\partial_T\rho(T_{wb} - T_0)), \quad (4)$$

where $\tau = C_{pr}\rho_r/C_{ps}\rho_s$, is less affected: for the conditions described in this case study, neglecting the rain temperature effect would overestimate it by only 16%.

The assumptions that a deep mixed layer was present at the onset of the rain and that the heat flux into the fossil mixed layer was negligible during the rain—that is, that the barrier layer inhibited any deeper mixing—are central to the interpretation of the observations. To support these assumptions, the mixed layer model

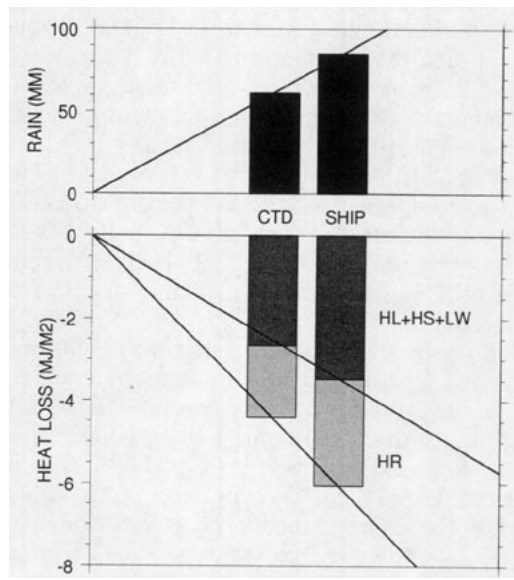

FIG. 7. Lower panel: partition of the net heat fluxes between rain and nonrain heat loss, as inferred from the CTD profile (left) and from the shipboard sensors (right). Upper panel: net freshwater input. The lines visualize the identical ratio between quantities inferred from the CTD profile and from the shipboard sensors.

of Price (1979) was run. This model has been extensively tested in similar highly stratified conditions. The vertical resolution was set at 2.5 cm and the time step at 0.001 day. The model was initialized with a mixed layer 22 m deep at 0000 UTC and forced by the observed heat flux, wind stress, and moisture flux. The rain heat flux was included, as well as the flux of horizontal momentum due to the raindrops ($\sim \rho_r \dot{d} U$), which, for a rain rate of 8×10^{-6} m s^{-1}, is as large as the bulk-parameterized wind stress of a $U = 5$ m s^{-1} wind. For both 3 September (30-mm rain input) and 4 September (85-mm rain input), the model output shows that 1) the barrier layer remained shallower than 3 m, with no deeper variations of temperature or salinity; 2) the barrier layer was completely eroded each day shortly after the rain stopped, before sunrise. An exact comparison between the modeled and observed $S(z)$ and $T(z)$, however, is not relevant, because ship mixing and interfacial waves perturbed the profiles in an unknown way.

Our observations confirm that the rain temperature must be taken into account when computing the net heat flux and the heat balance in the tropical ocean. Based on the observed heat deficit, the average rain heat flux in the ITCZ where the yearly rainfall reaches 3000 mm would be ~ 7 W m^{-2}. This is about 23% of the maximum net heat flux inferred by Gent (1991) for this area. Ignoring the rain heat flux would produce an erroneous heating of 1°C yr^{-1} for a mixed layer 54 m deep, which is far from negligible. The rain heat flux may not be important in global models, given the relatively small extent of the ITCZ, but it is crucial in the thermodynamics of mesoscale coupled ocean–atmosphere models of the Tropics, where considerable seasonal and interannual variability of rainfall, hence of rain heat flux, exist (cf. Janowiak and Arkin 1991).

The average heat flux error made assuming that the rain temperature equals the wet-bulb temperature, instead of the slightly colder temperature discussed by Gosnell et al. (1993), is at most 0.1 W m^{-2}, which is negligible compared to other sources of errors in heat flux measurements. Independent measurements of the rain temperature may not be necessary if humidity and/or bulb temperature are available.

Acknowledgments. Discussions with G. Barnes, C. Fairall, and R. Lukas, and comments by two anonymous reviewers, helped clarify this note. The authors would like to thank R. Knox and P. Niiler for their patience during our diversion from the official cruise objectives. R. Weller, R. Payne, and D. Hosom gave advice on the set up of the air–sea interactions system for the R/V *Moana Wave,* which was built and maintained by K. Bi, K. Constantine, R. Cunnigham, A. Goo, U. Knirsh, D. Myhre, H. Ramm, M. Simpson, C. Stephens, and C. Trefois. The plotting package *gri* by D. Kelley was used for all the figures. Work supported by National Science Foundation Grants OCE-8818732, REU-8900858, OCE-8922207, and OCE-9117078. SOEST Contribution 3586.

APPENDIX

Instruments and Data Processing

a. Hydrographic measurements

The CTD profiles were obtained using a SeaBird SBE-9 with ducted sensors. The time series were sampled at 12 Hz and lagged to account for the distance between the temperature and conductivity sensors. No averaging was done. The T–S loops due to ship heave and roll affecting the flow through the pumped duct were edited out. The calibration is described in Trefois et al. (1993). The CTD was lowered at 0.3 m s^{-1} from the starboard A-frame of the R/V *Moana Wave* to achieve a high vertical resolution near the surface.

b. Meteorological measurements

Precision meteorological sensors were mounted 12 m above sea level on a retractable steel tower aligned with the bow of the ship, where the airflow is least perturbed by the ship's superstructures.

Wind velocity was measured by a pair of vector-averaged R. M. Young vane/impeller wind meters, transformed to earth coordinates using the ship's gyrocompass and the velocity over water from the ADCP.

Rain rate was measured by a Scientific Technology optical scintillation gauge, the integral of the rain rate being constrained by an R. M. Young capacitance siphon gauge. The residual cross-calibration error was 3 mm rms.

Absolute humidity was measured by an Ophir infrared absorption hygrometer mounted in free air, and relative humidity by a pair of Rotronics capacitance hygrometers mounted in R. M. Young aspirated radiation shields. The hygrometers were calibrated against General Eastern dewpoint sensors after the cruise. Wet-bulb temperatures were computed using equations from the Smithsonian Meteorological Tables. The offset between the Rotronics wet bulbs was 0.2°C, $\sigma = 0.1$°C, and the offset between the average of the two Rotronics and the Ophir wet bulbs was 0.1°C, $\sigma = 0.2$°C. Despite the rapidly varying rain and relative humidity, the instruments were providing wet-bulb temperatures consistent within 0.2°C. Since the Ophir was noisy during rain, the average of the two Rotronics was used to compute the evaporative and latent heat fluxes.

Air temperature was measured by a platinum resistance thermometer mounted in an aspirated radiation shield. Additional temperature measurements were provided by the platinum resistance thermometers built in the Rotronics, by a thermistance in the Ophir, and by thermistances in the pyrgeometer. These sensors were cross-calibrated over 3 h on a cloudy night on 29

August, with ~ 7 m s^{-1} wind and no precipitation, when their temperatures can be expected to be quite close. The standard deviation of the average temperatures of the six sensors was 0.15°C. The time series from the platinum resistance thermometer was shifted to the median of the sensors to compute the sensible heat flux.

Incoming solar radiation was measured by an Eppley PSP pyranometer. Incoming longwave radiation was measured by an Eppley PYR pyrgeometer, the dome and base temperatures of the pyrgeometer being separately recorded. Both radiometers were factory-calibrated before the cruise.

The sensors were digitized at 1 Hz by a Campbell Scientific CR-7, and recorded on a Sun Microsystems workstation. The time series were low-pass filtered and decimated to a sampling period of 5 min during post-processing. In addition, sea surface temperature was measured at 4-m depth by a thermistance in the ADCP transducer, calibrated against the CTD to an accuracy of ~ 0.1°C. Because the upper layer is mixed by the hull of the ship while underway, the 4-m depth temperature corresponds to an average temperature over the upper 5 m or so.

The wind stress was parameterized following Smith (1988). The sensible and latent heat fluxes were parameterized from the bulk measurements using the coefficients from Liu et al. (1979). The net shortwave radiation flux was computed assuming an albedo of 0.04. The net longwave radiation flux was computed following Dickey et al. (1994). The sensible heat flux due to the rain was computed assuming that the rain temperature was the wet-bulb temperature [cf. Eq. (3)]. Fluxes heating the ocean are conventionally positive.

REFERENCES

Austin, D. M., and S. G. Geotis, 1980: Precipitation measurements over the ocean. *Air–Sea Interactions: Instruments and Methods,* F. Dobson, L. Hasse, and R. Davis, Eds., Plenum Press, 523–541.

Bahr, F., and C. Paulson, 1990: The effects of rainfall and diurnal heating on temperature and salinity in the upper five meters of the equatorial Pacific. *Eos, Trans. Amer. Geophys. Union,* **71,** 1401. [Abstract only.]

Dickey, T. D., D. V. Manov, R. Weller, and D. A. Siegel, 1994: Determination of longwave heat flux at the air–sea interface using measurements from buoy platforms. *J. Atmos. Oceanic Technol.,* **11,** 1057–1078.

Gent, P., 1991: The heat budget of the TOGA-COARE domain in an ocean model. *J. Geophys. Res.,* **96,** 3323–3330.

Gosnell, R., C. W. Fairall, and P. J. Webster, 1993: The temperature of and the sensible heat due to rain in TOGA-COARE. *Eos, Trans. Amer. Geophys. Union,* **74,** 43(Suppl.), p. 125. [Abstract only.]

Greenhut, G. K., 1978: Correlations between rainfall and sea surface temperature during GATE. *J. Phys. Oceanogr.,* **8,** 1135–1138.

Janowiak, J. E., and P. A. Arkin, 1991: Rainfall variations in the Tropics during 1986–1989, as estimated from observations of cloud-top temperature. *J. Geophys. Res.,* **96,** 3359–3373.

Kincaid, D. C., and T. S. Longley, 1989: A water droplet evaporation and temperature model. *Trans. ASAE,* **32,** 457–463.

Kinzer, G. D., and R. Gunn, 1951: The evaporation, temperature, and thermal relaxation-time of freely falling water drops. *J. Meteor.,* **8,** 71–83.

Liu, W. T., K. B. Katsaros, and J. A. Businger, 1979: Bulk parameterization of air–sea exchanges of heat and water vapor including the molecular constraints at the interface. *J. Atmos. Sci.,* **36,** 1722–1735.

Lukas, R., 1990: Freshwater input to the western equatorial Pacific Ocean and air–sea interaction. *Air–Sea Interaction in the Tropical Western Pacific, Proc. Beijing, China, US-PRC Int. TOGA Symp.* China Ocean Press, 305–328.

——, and E. Lindstrom, 1991: The mixed layer of the western equatorial pacific ocean. *J. Geophys. Res.,* **96,** 3343–3358.

Ostapoff, F., Y. Tarbeyev, and S. Worthem, 1973: Heat flux and precipitation estimates from oceanographic observations. *Science,* **180,** 960–962.

Price, J. F., 1979: Observations of a rain-formed mixed layer. *J. Phys. Oceanogr.,* **9,** 643–649.

Smith, S. D., 1988: Coefficients for sea surface wind stress, heat flux and wind profile as a function of wind speed and temperature. *J. Geophys. Res.,* **93,** 15 467–15 472.

Trefois, C., P. Flament, R. Knox, and J. Firing, 1993: CTD hydrographic data from the Moana Wave cruises MW-9010 and MW-9012. School of Ocean and Earth Science and Technology, Tech. Rep. SOEST-93-01, University of Hawaii, 157 pp.